Coal Operators' Conference

Faculty of Engineering and Information
Sciences

2011

Numerical Simulation of the De-stressed Deformation of Mining Coal Strata at Different Pore Pressures

Hongyong Liu
China University of Mining and Technology, China

Yuanping Chen
China University of Mining and Technology, China

Haidong Chen
China University of Mining and Technology, China

Shengli Kong
China University of Mining and Technology, China

Qingwei Zhai
China University of Mining and Technology, China

Follow this and additional works at: https://ro.uow.edu.au/coal

Recommended Citation

Hongyong Liu, Yuanping Chen, Haidong Chen, Shengli Kong, and Qingwei Zhai, Numerical Simulation of the De-stressed Deformation of Mining Coal Strata at Different Pore Pressures, in Naj Aziz and Bob Kininmonth (eds.), Proceedings of the 2011 Coal Operators' Conference, Mining Engineering, University of Wollongong, 18-20 February 2019
https://ro.uow.edu.au/coal/379

NUMERICAL SIMULATION OF THE DE-STRESSED DEFORMATION OF MINING COAL STRATA AT DIFFERENT PORE PRESSURES

Hongyong Liu, Yuanping Cheng, Haidong Chen, Shengli Kong and Qingwei Zhai

ABSTRACT: Gas extraction from mining induced de-stressed areas is one of the most efficient and cost-effective methods for eliminating coal and gas outbursts in China. In the paper, the characteristics of fracture induced pressure relief at different pore pressures and confining pressures on the de-stressed deformation of strata are analysed by using FLAC software. A strain-softening constitutive relation was used and the confining pressure was unloaded after the model was loaded to reach a static equilibrium state. The numerical results show that under the same confining pressure, and with the increase of pore pressure, the deformation of strata due to de-stressing as well as the fracture zones also increase significantly, and the characteristics of fissure induced pressure relief becomes more apparent. For seams with high gas pressure, the impact of pore pressure on the deformation of mining disturbed strata cannot be neglected. The numerical results are in good agreement with field observations, and improve the development of the coupled gas-solid theory in mining induced de-stressed strata.

INTRODUCTION

Coal seams characterized by low gas permeability usually less than 2.5×10^{-4} md (0.01 m^2/ (MPa^2·d)), are regarded as the hard-to-drain coal seams in China. In order to drain coal gas efficiently, the coal seam permeability must be improved significantly. Various workers (Yu, 1986; Yu, 2005; Cheng, *et al.*, 2003; 2004; Yu and Cheng, 2007) and practices proved that pressure-relief gas drainage, especially the use of the protective seam and pressure-relief gas drainage from the protected layer, was one of the most effective and cost-effective regional methods to eliminate coal and gas outbursts and reduce gas content. *The Rules of Coal and Gas Outburst Prevention* (hereinafter referred to as *The Rules* were published in 2009 by the State Administration of Coal Mine Safety of China (SACMSC, 2009). Th*e Rules* require that the regional methods must be used as a priority for coal and gas outburst prevention, and local methods could be used as supplemental methods. The regional comprehensive methods, with the protected layer as priority selection, must be taken prior to the extraction of seams with outburst risk.

For different geologic conditions, the effects of gas control methods based on de-stressing can be different in the same coal field. Gas control methods should be selected to meet the depressurized effect and the requirement of *The Basic Indicator of Gas Drainage in Coalmine* (hereinafter referred to as The Indicator). Yuan (2005) showed that dilatational deformation could be used as the indicator of the depressurized effect for the protected layer, which related to the mining height of protective seam, roof control method, the dimension of the coal face and mining depth.

Much of the research work on the protective seam are based on physical-scale modelling or numerical calculations that are associated with geo-stress without due consideration of the pore pressure. When the gas pressure is high, the effective stress is much less than the total stress. Liang *et al.*, (1995) showed gas pressure could affect the mechanical strength of the coal mass. Thus, pore pressure could directly influence the mechanical response of coal and rock mass, and consequently the simulations without taking pore pressure into consideration could not reflect the real depressurized effect on the protected layer. This makes it difficult for the use of the protective layer, especially when choosing the protective layer and designing the drainage holes and other projects for coal and gas outburst prevention, which also influences the effectiveness, safety and economical efficiency of pressure-relief gas drainage. Various workers (Liang, *et al.*, 1995; Yao and Zhou, 1988; Zhao, 1992; Jin, *et al.*, 1991; Xu, *et al.*, 1993 and He, *et al.*, 1996) found that the changing of mechanical strength, mechanical response and deterioration is influenced by pore pressure. Lu *et al*. (2001) updated the Karl Terzaghi effective stress formula of porous media, found that the regulation of effective pore pressure coefficient changes the

National Engineering Research Centre of Coal Gas Control, China University of Mining and Technology, Xuzhou, Jiangsu 221008, China, ypcheng620924@163.com

complete stress-strain process. By using shear strain gradient plasticity theory, Wang and Pan (2001) established the relationship of stress and strain under the confining pressure and pore pressure. Yin and Wang (2009) and Wang *et al*. (2010) set up a coupled elastic-plastic damage constitutive model, and described the mechanical characters and behaviour of gas coal and rock at different loads. Using FLAC, Wang *et al*. (2009) numerically modelled a rock specimen with random defects in uniaxial plane strain compression, and investigated the effects of pore pressure on the failure processes, overall deformational characteristics and precursors.

In this paper, the characteristics of fissure induced pressure relief of mining coal mass at different pore pressures and confining pressures are analysed by using FLAC software. A strain-softening constitutive relationship is used and the confining pressure is unloaded after the model is loaded to reach a static equilibrium state based on the geological condition of Xinjing coal mine in Yangquan coal field.

RESEARCH METHODS

The hybrid discretization, dynamic relaxation method and explicit difference scheme was adopted. FLAC has the superiority for handling strain softening problems. It has been extensively used in mining coal and rock fracture analysis by various workers (Lan, *et al.*, 2008; Peng, 2008 and Gao, *et al.*, 2010). In FLAC, the pore pressure is described by effective stress law, and a positive value would be taken under the compressive condition. The relationship between effective stress σ' (negative when compressed), total stress σ_0 and pore pressure p could be described as:

$$\sigma' = \sigma_0 + \alpha p \tag{1}$$

Where, α is the effective gas stress coefficient.

Assuming that the mechanical behaviour of coal and rock mass follows the strain-softening constitutive relationship, coal and rock mass is in isotropy linear elasticity during elasticity stage; after the peak strength, the constitutive relationship of coal and rock mass is M-C shear and tensile damage combined strain-softening model. The frictional angle and cohesion become lower with the elastic shear strain, until the frictional angle and cohesion reach the residual values.

Numerical models

The computation model is a standard cylinder, with a radius of 25 mm and 100 mm in height. Divided into 8 000 units, the vertical displacement of the cylinder bottom is fixed, and a radial load is imposed around the cylinder and on the top, corresponding to the larger friction between the sample and the press heads.

The model calculation uses the strain-softening model by FLAC software. The physical properties of the model are defined as in Table 1. The initial cohesion is set at 2.0×10^6 Pa and the initial frictional angle is 41°, the relationship of cohesion, frictional angle with plastic strain is shown in Figure 1. The numerical models are divided into six schemes with pore pressures respectively set as 0, 0.2 MPa, 0.4 MPa, 0.6 MPa, 0.8 MPa, 1.0 MPa, 1.2 MPa, and 1.4 MPa.

Table 1 - Physical mechanics parameters of the numerical model

Density ρ (kg· m^{-3})	Young modulus E (GPa)	Poisson ratio μ	frictional angle φ (°)	Cohesion c (MPa)	Tensile strength σ_t (MPa)
2 400	1.63	0.21	41	2.0	1.41

Calculation steps

(1) After creating the unexcavated model, the constitutive relation, boundary conditions and load conditions (confining pressure and internal pore pressure) are defined, and numerical computations started until the maxmum unbalance force is less than 1.5×10^{-3} N.

(2) Using the Fish function to load the pressure on the sample top progressively, 100 kPa per section, and the static equilibrium would be disturbed by the loads.

(3) A new calculation process starts (FLAC adds a damping automatically) until a new static equilibrium state is reached.

Axial strain calculation

To study the effect of pore pressure on depressurized deformation of coal and rock mass, the numerical simulation will check and calculate the axial strain ε_a as in Figure 1 during the calculation process:

$$\varepsilon_a = \frac{u}{L} \qquad\qquad (2)$$

Where, u is the displacement of rock sample top, in m; L is the sample height, in m; ε_a is the axial strain, if it is positive, the sample is compressed.
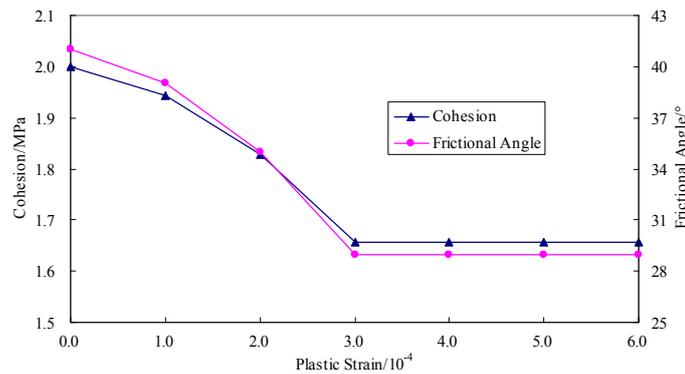

Figure 1 - Relations of cohesion and frictional angle among plastic strain

SIMULATION RESULTS

The compression experiments by cylindrical specimens are performed at different pore pressures under 1.0 MPa confining pressure, and induce the damage deformation at the pore pressures of 0, 0.4 MPa, 0.6 MPa, 0.8 MPa, 1.0 MPa, 1.2 MPa and 1.4 MPa. In order to compare the damage deformation at different confining pressures, another set of compression experiment is computed at the pore pressures of 1.2 MPa and 1.4 MPa under 2.0 MPa confining pressure.

Influence of pore pressures on failure process under fixed confining pressure

Figure 2 shows the relationship between axial stress and axial strain of testing a specimen at different pore pressures under 1.0 MPa of confining pressure.
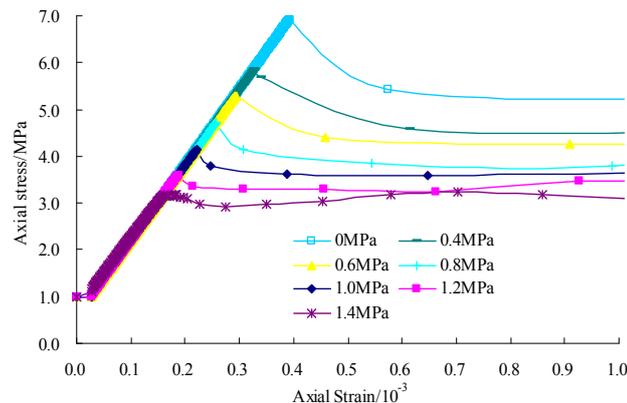

Figure 2 - Relationships between axial stress and axial strain of testing specimen at different pore pressures under 1.0 MPa confining pressure

It can be seen from Figure 2 that the peak stress of damage failure and its corresponding axial strain decreases with the rising pore pressure. The higher the pore pressure, the smaller the declining rate after peak stress, and the mechanical characteristics become brittle from plastic. When the pore pressure is zero, the peak stress reaches 6.92 MPa and its corresponding axial strain is 3.94×10^{-1}. After the peak

stress, the residual stress drops down to 5.44 MPa, falling 21.4%. While the pore pressure is increased to 1.4 MPa, the peak stress reaches 3.17 MPa and its corresponding axial strain 1.6×10^{-1}. But the residual stress is only down to 3.15 MPa after the peak stress, falling 0.63%. After the specimen has damaged, some plastic strain is caused by the larger load increment. Those observations demonstrated some related conclusions by Wang (2007) and Liang *et al*. (1995).

Influence of pore pressures on failure process under different confining pressures

The relationship between axial stress and axial strain of the testing specimen at different confining pressures under the same pore pressures 1.0 MPa and 2.0 MPa, can be shown in Figure 3.
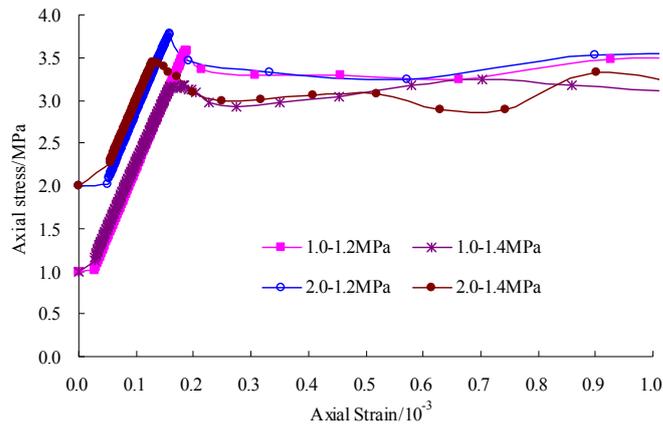

Figure 3 - Relationships between axial stress and axial strain of testing specimen at different confining pressures under the same pore pressures

As it can be seen in Figure 3 the peak stress and the brittleness of specimen increases with increasing confining pressure, but the axial strain corresponding to peak stress becomes lower. Under 1.4 MPa pore pressure, when the confining pressure increases from 1.0 MPa to 2.0 MPa, the peak stress reaches 3.78 MPa from 3.58 MPa, and its corresponding axial strain drops to 1.59×10^{-1} from 1.87×10^{-1}. While the pore pressure is 1.4 MPa, the peak stress rises to 3.45 MPa from 3.18 MPa, and its corresponding axial strain also drops to 1.31×10^{-1} from 1.82×10^{-1}, and residual stress is 2.92 MPa and 2.99 MPa respectively.

Influence of pore pressure on depressurized deformation of coal mass

Plastic zone contains shear yield zone and tensile yield zone in FLAC. The plastic zone distribution at 0 and 1.4 MPa pore pressure under 2.0 MPa confining pressure is shown in Figure 4 (a) and (b).
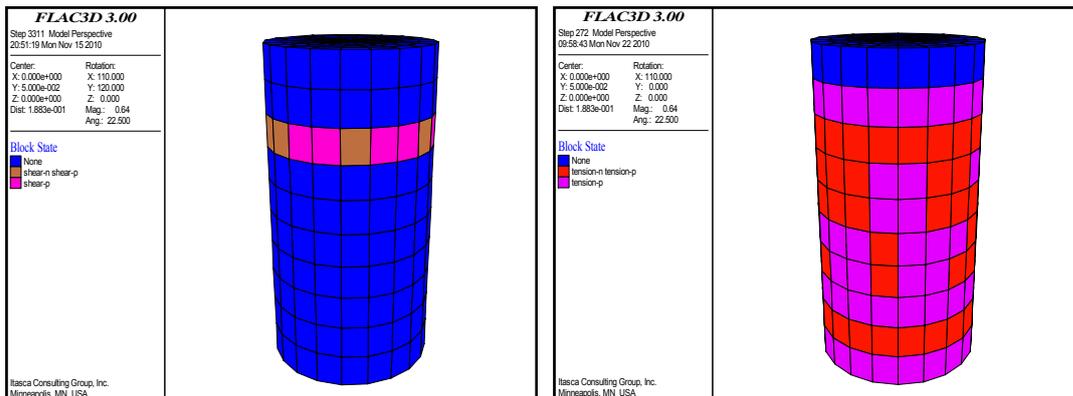
(a) pp=0 MPa at 3311 steps   **(b) pp=1.4 MPa and 272 steps**

Figure 4 - Distributions of yielded elements at different pore pressure and time step under 2.0 MPa confining pressure

The results indicate that when the confining pressure is fixed, the specimen only has shear fracture under the 0 pore pressure in the compression experiment. In Figure 4 (a), the specimen has tensile failure

caused by stress concentration in adjacent units, while the pore pressure rises to 1.4 MPa from 0. The tensile failure appears at the ends of fissure under the pore pressure, caused by the tensile stress concentration for gas-filled coal containing cracks, according to the Griffith Strength Theory. Therefore, those simulation results agree with the theory and some related calculations as shown by Liang *et al*. (2010).

SIMULATION CASE STUDIES

In order to investigate the influence of pore pressure on depressurized failure and deformation, the remote protective layer exploitation was simulated at different pore pressures.

Computation model

The computation models are based on the geological features of a Xinjing coalmine. The geometrical characteristics, meshing and boundary conditions are shown in Figure 5.
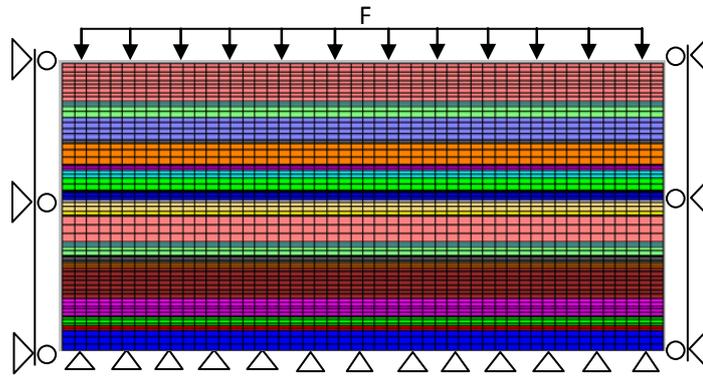

Figure 5 - Geometry features and boundary conditions of model

The computation model has a dimension of 500 m × 210 m with an excavation length of 300 m in the No.3 coal seam. The horizontal displacement is fixed except the bottom and the top. The numerical calculation uses a large deformation mode. The burial depth of No.15 coal seam is 380 m, and the physical properties of the coal and strata in the simulation are shown in Table 2.

Table 2 - Physical mechanics parameter of the coal and rock seams in the model

No.	Name	Thick-ness (m)	Summation (m)	Bulk modulus K (GPa)	Shear modulus G (GPa)	Frictional angle φ (°)	Cohesion c (MPa)	Tensile strength T (MPa)	Cohesion softening slop Ck (GPa)	Frictional angle softening slop Fk (10^4(°))
1	Medium sandstone	27	210.3	27.4	18.8	38	6.4	4.17	0.573	2.0
2	Mudstone	3.4	183.3	1.80	0.929	30	2.67	2.50	0.426	1.5
3	Sandy mudstone	7.8	179.9	2.03	1.04	33	3.2	3.34	0.573	2.0
4	Coal	2.6	155.5	2.58	1.19	26	1.23	1.28	0.426	1.5
5	Limestone	3.2	66.7	10.5	6.91	37	4.7	6.83	0.573	2.0

Using the FISH function, the units in the mining area are deleted step by step. After deleting the units, the model will not maintain the equilibrium state under the pore pressure and the confining pressure. The model is recalculated until the unbalanced force is less than the defined value. The simulations are divided into three schemes with pore pressure 0, 1.0 MPa and 1.7 MPa.

Simulation results

The vertical stress on No.3 coal seam floor and the vertical relative deformation of the whole No.3 coal seam at different pore pressures are shown in Figures 6 and 7, when the protective layer has advanced 200 m.
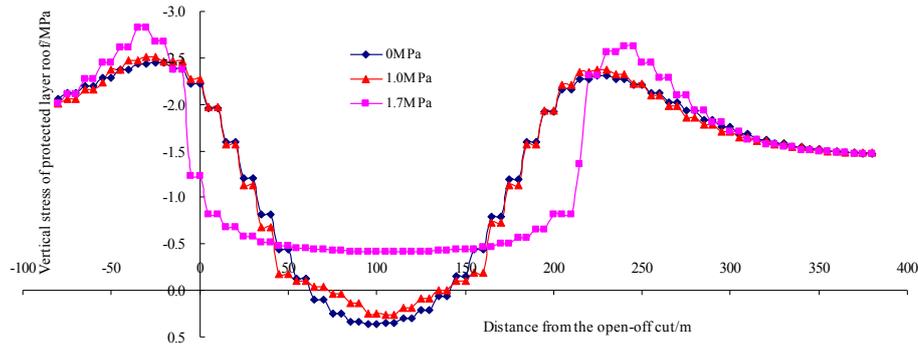
Figure 6 - Curves of vertical stress on No.3 coal seam floor at different pore pressure

As discussed previously, the peak stress of yield damage and its corresponding axial strain decrease with the rising pore pressure, and the mechanical characteristics become brittle from plastic. The peak stress concentration is increased with the rising pore pressure after a certain distance of the protected layer being mined, shown in Figure 6. As shown in Figure 7, the range of the dilatational deformation area and the deflection also increased, which causes significant compression in the coal block.

After the protected layer advanced 200 m, the depressurized length of protected layer is 160 m at the pore pressure 0. In the most depressurized zone, the stress became tensile from compressive at 0.364 MPa, and corresponding relative deformation is 1.3‰. The peak concentration stress in the both sides of the coal block reaches -2.45 MPa, and the stress concentration factor is 1.63, and corresponding compression deformation -1.4‰ at 20 m to the edge of coal seam. While the pore pressure rose to 1.7 MPa, the depressurized length increased to 220 m, the minimum stress is -0.417 MPa, i.e., about 27.8% of the initial value, and the depressurized deformation reached 81.2‰ in the most depressurized zone. Meanwhile, the peak concentrated stress at 45 m to the edge of coal block reached -2.62 MPa, and the stress concentration factor 1.75, the max compression deformation is -1.0‰, and the value of above parameters is in the same order of magnitude as the 0 while the pore pressure is increased to 1.0 MPa.
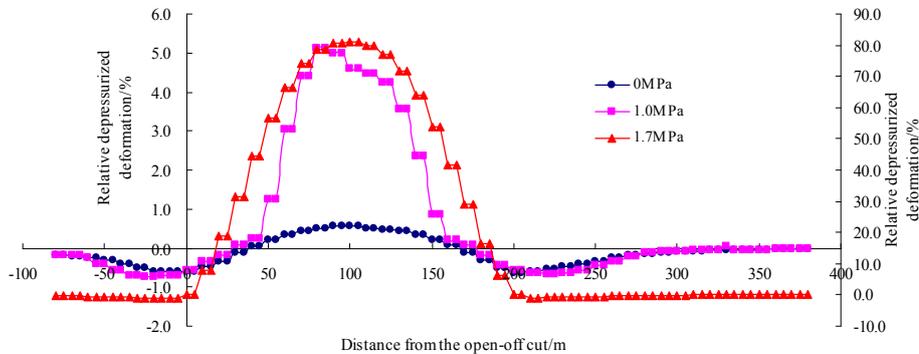

Figure 7 - Curves of vertical relative deformation of No.3 coal seam at different pore pressure

These results showed that the depressurized deformation and the damaged area increased with the rising pore pressure. And the characteristics of depressurized fissure are also becoming more obvious. The stress concentration in both coal seams becomes higher, and the distance from the stress concentration zone to the edge of coal block is also larger. If the pore pressure is not considered, the depressurized effect and the position of peak stress concentration would be underestimated. This will have a hidden danger to the design of gas control projects and the safe mining of protected layer. Obviously when the pore pressure reaching a certain value, the effect of pore pressures on the depressurized deformation of coal mass cannot be neglected.

Simulation results also indicated that the height of the water-conducting crack zone (zone and fissure zone) is over 135 m, which means that the No.3 coal seam, locating above the fissure zone of No.15 coal seam, will have well-developed fractures and increased permeability, therefore the effect of pressure-relief gas drainage can be achieved.

CONCLUSIONS

Based on the systematic studies of mechanical characteristics of coal and rock mass due to mining, the following conclusions can be reached:

(1) The peak stress of damage failure and its corresponding axial strain decreases with the rise of pore pressure, when the confining pressure is fixed. The higher the pore pressure, the smaller the rate of reduction after peak stress, and the mechanical characteristics become brittle from plastic.

(2) When the confining pressure is fixed, on shear fracture occurs under the 0 pore pressure in the compression experiment. The specimen has tensile failure caused by stress concentration in adjacent units, as the pore pressure increases to 1.4 MPa from 0.

(3) The simulation based on protective layer exploitation in Yangquan Xinjin coal mine shows that the depressurized area, the peak stress concentration and the position increase with the rising pore pressure after a certain distance of protected layer have been mined. When the pore pressure reaches a certain value, the effect of pore pressure on the depressurized deformation of coal mass must be considered.

(4) As the numerical simulation shown, No.3 coal seam located above the fissure zone of No.15 coal seam. After the mining of protective seam, mining induced cracks can be well-developed with enhanced permeability in the protected seams, thus facilitating the practice of efficient gas drainage.

(5) The numerical results are in good agreement with field observations, which improve the gas-solid coupled theory of mining coal mass.

ACKNOWLEDGMENT

REFERENCES

Cheng Y P, Yu Q X, Yuan L, 2003. Gas extraction techniques and movement properties of long distance and pressure relief rock mass upon exploited coal seam, in *Journal of Liaoning Technical University*, 22(4), pp 483-486.

Cheng Y P, Yu Q X, Yuan L, Li P. Li Y Q, Tong Y F, 2004. Experimental research of safe and high efficient exploitation of coal and pressure relief gas in long distance, in *Journal of University of Mining and Technology of China*, 33(2), pp 132-136.

Gao F Q, Kang H P, Lin J, 2010. Numerical simulation of zonal disintegration of surrounding rock mass in deep mine roadways, in *Journal of China Coal Society*, 35(1), pp 21-25.

He X Q, Wang E Y, Lin H Y, 1996. Coal deformation and fracture mechanism under pore gas action, in *Journal of China University of Science and Technology*, 25 (3), pp 6-11.

Jin Z M, Zhao Y S, He J E, Zhang M T, 1991. An experimental study on the mechanical properties of gas-bearing coal seams, in *Chinese Journal of Rock Mechanics and Engineering*, 10(3),   pp 271-180.

Liu H Y, 2010. Fully coupled model and engineering application for deformation and pressure-relief gas flow of remote coal and rock mass due to mining, PhD thesis, China University of Mining and Technology, Xuzhou.

Liu H Y, Cheng Y P, Zhao C C, Wang H F, Chen H D, 2010. Constitutive model for elasto-brittle-plastic damage of coal rock mass due to mining and its application, in *Chinese Journal of Rock Mechanics and Engineering*, 29(2), pp 358-365.

Lu P, Sheng Z W, Zhu G W, Fang E C. The effective stress and mechanical deformation and damage characteristics of gas-filled coal, in *Journal of University of Science and Technology of China*, 31(6), pp 686-693.

Lan H, Yao J G, Zhang H X, Xu N Z, 2008. Development and application of constitutive model of jointed rock mass damage due to mining based on flac3d, in *Chinese Journal of Rock Mechanics and Engineering*, 27(3), pp 572-579

Liang B, Zhang M T, Pan Y S, Wang Y J, 1995. The experimental research on the effect of gas on mechanical properties and mechanical response of coal, in *Chinese Journal of Geotechnical Engineering*, 17(5), pp 12~18.

Peng Y W, 2008. Study of evolution of mining-induced fractures field and its coupling effect with gas seepage under the conditions of high-strength underground mining, PhD Thesis, China Coal Research Institute, Beijng.

State Administration of Coal Mine Safety of China, 2006. *Basic index of coal mine gas drainage and exploition (AQ1026-2006)*. China Coal Industry Publishing House: Beijing.

State Administration of Coal Mine Safety of China, 2009. *Rules of coal and gas outburst prevention*. China Coal Industry Publishing House: Beijing.

Wang X B, 2007. Effects of pore pressure on failure process and axially deformational characteristic for rock specimen with random material imperfections, in *Proceedings of the 12th International Symposium on Water Rock Interaction, W R I 212,* pp 1421-1425 (Taylor and Francis Group London).

Wang X B, Pan Y S, 2001. Theoretical analysis of relationship between stress and strain in consideration of confining pressure and pore pressure of rock sample, in *Journal of Geomechanics*, 7(3), pp 265-270.

Wang X B, Wang W, Pan Y S, 2010. Numerical simulation of the strain localization of the surrounding rock of a circular tunnel at different pore pressures, in *Journal of China Coal Society*, 35(5),   pp 723-728.

Wang D K, Yin G Z, Liu J, Wang F B, Qin H, 2010. Elastoplastic damage coupled model for gas-saturated coal under triaxial compression, in *Chinese Journal of Geotechnical Engineering*, 32(1):55-60.

Wang X B, Zhao F C, Pan Y S, 2009. Failure processes and overall deformational characteristics of rock specimen with random imperfections at different pore pressures, in *Journal of Disaster Prevention and Mitigation Engineering*, 29(1), pp 1-8.

Xu J, Xian X F, Du Y G, Zhang G Y, 1993. An experimental study on the mechanical property of the gas-filled coal, in *Journal of Chongqing University*, 16(5), pp 42-47.

Yu B F, 1986. *Cognition and Practice on the Exploitation of the Protective Layers*, China Coal Industry Publishing House, Beijing.

Yuan L, 2005. *Theory and Technology of Methane Extraction in Multiseams of Low Permeability*, China Coal Industry Publishing House, Beijing.

Yu Q X Effect examination on remote protective layer exploitation in Tianfu coalmine, in *Theory and Engineering Practices on Prevention and Control for Gas Disasters in Coal Mines*. China University of Mining and Technology Press, Xuzhou.

Yu Q X, Cheng Y P, 2007. Development of regional gas control technology for Chinese coalmines, in *Journal of Mining* and *Safety Engineering*, 24(4), pp 389-392.

Yin G Z, Wang D K, 2009. A coupled elastoplastic damage model for gas-saturated coal, in *Chinese Journal of Rock Mechanics and Engineering*, 28(5), pp 993-999.

Yao Y P, Zhou S N, 1988. The mechanical property of coal containing gas, in *Journal of University of Mining and Technology* of *China*, 17 (1), pp 1-7.

Zhao Y S, 1992. Research on coupling effect of two-phase coal and gas, PhD thesis. Tongji University, Shanghai.